Aldoumani et al., *Cogent Engineering* (2016), 3: 1225879
http://dx.doi.org/10.1080/23311916.2016.1225879

cogent engineering

MATERIALS ENGINEERING | RESEARCH ARTICLE

The robustness of carbon fibre members bonded to aluminium connectors in aerial delivery systems

Nada Aldoumani[1]*, Hamed Haddad Khodaparast[1], Ian Cameron[1], Michael Friswell[1], David Jones[2], Arun Chandrashaker[1] and Johann Sienz[1]

Received: 30 June 2016
Accepted: 14 August 2016
First Published: 24 August 2016

*Corresponding author: Nada Aldoumani, The Advanced Sustainable Manufacturing Technologies (ASTUTE) Project, College of Engineering, Swansea University, Fabian Way, Swansea SA1 8EN, UK
E-mail: n.s.f.aldoumani@swansea.ac.uk

Reviewing editor:
Wei Meng, Wuhan University of Technology, China

Additional information is available at the end of the article

Abstract: In this paper a framework for robust design solution of an adhesively bonded joint between a composite material and an aluminum connector is developed. To this end, an approach has been developed to automate the process of robust design by linking Ansys workbench and an in-house MATLAB code. The model employed in this study investigated the possibility of joining composite materials to aluminum components which is a problematic process in terms of preparation, implementation, etc. Before designing such a join, it is necessary to fully understand the behaviour of the proposed aluminum connector with the carbon fibre member. To achieve this, the investigation of the adhesive layer's behaviour and the uncertainties involved in such structures was identified. The behaviour of the adhesive between the carbon fibre composite and the aluminum connector was modelled based

ABOUT THE AUTHORS

Nada Aldoumani is an engineering doctorate (EngD) candidate at Swansea University. She has obtained her postgraduate degree in Structural Engineering from Cardiff University in 2010. She is heavily involved in ANSYS Work Bench, APDL, ACP, MATLAB coding and Composite materials. Her EngD work involves studying the uncertainty in composite structures that are adhesively bonded to dissimilar materials.

Hamed Haddad Khodaparast is currently a senior lecturer in Engineering at Swansea University. He obtained his PhD degree from University of Liverpool in 2010. He has many publications on uncertainty analysis and optimisation studies in aerospace engineering and structures.

Ian Cameron is currently a senior project officer conducting research for the ASTUTE 2020 Operation in College of Engineering at Swansea University. He obtained his PhD from Swansea University in 2000.

Micheal Friswell is a professor of Aerospace structure at Swansea University.

David Jones is currently an engineering manager for Airborne Systems Ltd. He is involved in the design and manufacture of Aerial Delivery Systems.

Arun Chandrashaker is a graduate engineer from Swansea University.

Johann Sienz holds a personal chair in the College of Engineering, Swansea University, where he is the deputy head of College and the director of Innovation and Engagement.

PUBLIC INTEREST STATEMENT

This research paper discusses a common problem in engineering applications that is called engineering design including parametric uncertainty. In other words, any material will have a certain amount of uncertainty in its properties and this can result from the processing, composition or the anisoptropic nature of the material as in composites. The current work investigates the uncertainty involved in joining a carbon fibre tubes via aluminium connectors. In this case, the thickness of the adhesive layer between these two dissimilar materials will be uncertain in terms of the resulting debonding force and sliding distance that will cause failure of the joint. This requires assumptions of the various possible thicknesses of the adhesive layer that will provide the optimum strength of the joint. The novelty of the current work involves the use of an automated method that is able to input a random number of thickness possibilities, i.e. hundreds or thousands, upon which the strength of the joint can be evaluated. Then, a selective tool can choose the optimum thickness that is able to provide the best joint strength and minimum sliding distance to keep the connector in place. This approach is applicable to any engineering application that involves a set of uncertain parameters that needs optimisation in order to provide the best set of parameters to achieve the goal of the application.

on the assumption that this layer acts as a "spring system" within a "cohesive" zone. Initially, the properties of Permabond ET5428 BLACK adhesive were used for validating the finite element model using the obtained test data. A robust design method is then employed to identify the right adhesive for the joint which not only maximizes the debonding force and sliding distance but is also robust with respect to the variation in its mechanical properties. A wide range of adhesive properties have been employed and a robust design technique based on uncertainty analysis is proposed.

Subjects: Aerospace Engineering; Industrial Engineering & Manufacturing; Mechanical Engineering; Materials Science

Keywords: cohesive zone; carbon fibre aluminium connector; adhesive joints; robust design; innovative design and manufacturing

1. Introduction

The frame of the current steel aerial delivery systems for air to ground delivery of equipment is robust enough to withstand the drag forces encountered while the frame, which is connected to a parachute from the top and equipment from the bottom, is descending to the ground. The descent results in tensile stresses in some members of the frame and compressive stresses in the remaining part of the frame. In addition, impact loads take place as the frame hits the ground. It is expected that the proposed replacement of materials will significantly reduce the mass of the frame which, in turn, will reflect on the total mass carried inside the aircraft. In the long term, this will reduce the fuel consumption of the delivery plane as well as allowing it to travel at higher speeds, due to the reduced mass of delivery equipment. Carbon fibre tubes can be used to replace steel members in a wide range of engineering applications. Their superior mechanical properties mean that a tube of the same weight as a steel tube can be much stronger, or a tube of the same strength can be much lighter. This might be applicable to the aerial delivery system by replacing the steel structure with carbon fibre-based composite tubes connected via aluminum connectors with the aid of an adhesive material applied to the interfacial area between the tube and the connector, i.e. the carbon fibre and the aluminum. However, in the design of this proposed structure, uncertainty factors should be considered in order to ensure robustness. In particular, the adhesive which connects the two materials is one of the major sources of uncertainties. To account for this, a detailed study of the adhesive properties and their representation in a Finite Element (FE) model should be conducted. The FE code is linked with an in-house MATLAB code to control uncertainty factors and determine the 'robust' optimal design.

Background research suggests that prior to adhesively bonding the aluminum to the composite material, the surface of the aluminum has to be pretreated in a chromic acid etch solution (CAE) according to DEF STAN 03–2/issue 3. Moreover, the surface of the composite material has to be degreased with acetone. This will ensure that both surfaces are clean and ready to be joined by applying the adhesive material. Afterwards, the joint has to be cured for 1 h at 120°C (Liljedahl, Crocombe, Wahab, & Ashcroft, 2007). When the adherends of the joint are made of different geometries and/or mechanical properties, the joint is referred to as "unsymmetric" or "unbalanced". The assessment of such joints has been widely studied by researchers (Zou, 2004). The most widely used model to simulate and predict the behaviour of such joints is the cohesive zone model (CZM) of single lap joints applied to joints made of aluminum bonded to composite materials (Liljedahl et al., 2007).

Generally, the failure of structures initiates at the weakest points where the parts are normally joined together. This means that reducing the number of joints will provide a robust structure which highlights the importance of the design of such structures. However, joints cannot be always avoided and therefore such joints must be carefully designed to ensure satisfactory strength. Mechanical joints are those which contain bolts, pins or rivets and can be found in both metals and composites. These types of joints are simple and suitable for structures where disassembly is required. However, the fastener

holes in such mechanical joints introduce an initiation site for micro and/or local damage to composite laminates during the manufacturing process as well as a location of stress concentrations in metals. These will result in strength degradation and premature failure of such structures (AHN, 2011).

Adhesive bonds compete with mechanical joints in their strength and efficiency. Moreover, the fastening holes and fasteners which are sources of stress concentration and weight increase are eliminated in such joints. In terms of stress distribution along the lap, studies have found that the stress is relatively uniform compared to mechanical joints. Despite these advantages, some drawbacks exist in adhesively bonded joints such as the difficulty of disassembling the joint if needed, the sensitivity of the joint strength on the environmental factors such as humidity and temperature and the surface preparation of such joints is costly and time consuming. In addition, the design of adhesively bonded joints with composite adherends is difficult due to the lack of a known failure criteria and the relatively low inter-laminar strength of the composite material (Baker, Dutton & Kelly, 2004). This means that such joints require careful design approaches and uncertainty studies to assess their suitability and reliability for engineering applications. A literature review has shown that most researchers have assessed only adhesively bonded joints of similar adherends which has initiated the drive to carry out an assessment of unsymmetric and unbalanced joints made of aluminum and composite materials in the current paper.

In this regard, a closed form continuum approach has been introduced by Hart-Smith in order to assess the stress distribution and the influence of various factors on the strength of the adhesively bonded single lap joints (SLJ) (Hart-Shith, 1973). Harris and Adams (1984) have also studied the stress distribution within the adhesively bonded joints using finite element (FE) models to predict the failure of single lap joints. Their method considered the elastic-plastic behaviour of the employed adhesive material utilising the maximum principal stress (or strain) criteria. Another study by Tsai, Morton and Matthews (1995) investigated the effect of the spew fillet on the adhesive stress distribution in laminated composite SLJs. It was found that the spew fillet pronouncedly reduces the shear and peel strength of the joint in agreement with other literature studies using the same principles (Lang & Mallick, 1998).

The static and fatigue behaviour of adhesively bonded joints of sheet moulding compound composite adherends were studied by Mazumdar and Mallick (1998). The failure load of the joints is shown to increase with either an increase in the overlap length or an increase of the thickness of the adhesive layer. The stress and strain distributions within the thickness of the adhesive layer in SLJs was investigated by Sullivan and co-workers (Li, Lee-Sullivan & Thring, 2000) who stated that the tensile peel and shear stresses at the free ends of the bond line were shown to noticeably change across the thickness of the adhesive. A study led by Kairouz, and Matthews (1993) examined SLJs with cross-ply adherends and showed that the surface layer orientation significantly affects the failure mode and strength of such joints. This study also revealed that the failure load increased as the ratio of the overlap length to the thickness of the adhesive increased. The influence of the bonding methods on the failure mode and strength of SLJs involving composites has been investigated (Kim, Yoo, Yi, & Kim, 2006). It was found that the failure strength was not always dependent on the adhesion strength of the adhesive.

In a study to assess adhesively bonded joints, tests were carried out to evaluate the strength of SLJs made of carbon fibre composites bonded to aluminum sheets utilising two different adhesive materials: film and paste types. In this study, three types of joints were considered, namely: adhesively bonded joints, fastener bolted joints and hybrid joints (i.e. made of adhesive-bolt assembly). The first outcome was that the strength of the hybrid joints with film adhesives (type FM73) were dominated by the strength of the adhesive itself. On the other hand, the strength of the hybrid joints with paste type adhesive (EA9394S) were mainly influenced by the bolt joint. This means that the hybrid joint is strong when the mechanical fastening by bolts is stronger than the adhesive whereas it is less effective when the bolt strength is less than the strength of the adhesive (Kweon, 2006). In a separate study, results have shown the stiffness of the joint is more affected by the response of the adherends to the test temperature rather than by the modulus of the thin adhesive layer. Moreover,

it was revealed that the theoretical models are able to predict the joint stiffness and rate of stiffness reduction with crack growth. The correlation which best simulates this fact was that applied to a rigid adhesive joint tested at −40°C wherein the fracture mode was purely cracking in the adhesive layer The available standards (see below standards) for testing bonded shear joints only employ short-bond laps which do not necessarily represent real-life engineering applications. For this reason, long lap joints have to be studied as they are more practical along with their greater efficiency when employed in structures (Owens, 2000). A relevant study by Matthews (Hollaway, 1994) has stated that the length of the lap joint and the thickness of the adherend greatly affect the strength of the joint and its structural efficiency. In his study, he stated that the optimum lap length (L) to the adherend thickness (t) should be 50/1 in order to obtain a joint strength of 70% more than the strength of the weakest adherend in the joint (Hollaway, 1994; Mathews, 1987). Another study by Campilho, Banea, Pinto, Da Silva, and De Jesus (2011) has shown that using Cohesive-zone models (CZMs) have already proved to be an effective tool in modelling the damage growth. Similarly, Xu and Wei (2012) has also employed the CMZs to study the overall strength and interface failure mechanisms of single lap joints. A detailed investigation on the post-buckling behaviour of adhesively bonded stiffened panels subjected to in-plane shear loading has been carried out (Villani et al., 2015). This has involved an experimental programme to determine the buckling load, buckling shape, collapse load and failure modes of two bonded stiffened panels. A nonlinear finite element based modelling approach, accounting for geometrical and material nonlinearities as well as progressive failure in the adhesively bonded interface between the skin and the stiffener has been proposed to predict the structural behaviour of the panels up to failure. This approach models the bonded interfaces using a newly developed cohesive zone based constitutive damage model. On the other hand, a finite element method has been employed by Hosseini-Toudeshky, Ghaffari, and Mohammadi (2013) to investigate the fracture analyses, crack growth trajectory and fatigue life of curved stiffened panels repaired with composite patches subjected to combined tension and shear cyclic loadings. For this purpose, finite element modeling has been performed for consideration of real 3-D crack-front in general mixed-mode conditions. Contact elements were used between the crack surfaces on two crack sides to prevent interferences of crack surfaces and a complementary program was developed to handle the automatic fatigue crack growth modeling. The effects of various patch layups and shear–tension loading ratios on fracture parameters of repaired aluminum panels were investigated. The use of composite materials in the aerospace industry is expanding and this is shown in the Boeing Dreamliner 787 (about 50% of materials used is CFRP), Airbus A350 which contains a similar proportion of composites in addition to Airbus A380 which now uses induction welded composite structures. This means that the market of composite materials is enormously expanding in the aerospace industry and other engineering applications which require further research on the capabilities of these materials for such applications (Degenhardt, 2014; Pappadàa, 2015).

Further to what is presented in the literature, this paper presents a robust design methodology for an aluminum/composite joint. The general drawbacks of adhesively bonded joints in terms of the associated uncertainty and variability of properties can be minimised through the selection of an optimal design for the joint along with the optimum properties of the adhesive material. This paper introduces a technique which enables the selection of the optimal and robust parameters for the joint and the adhesive material. This is based on running a model that contains a wide matrix of adhesive properties and identifying the parameters that provide the maximum debonding force and sliding distance. This paper introduces a framework for robust design of adhesively bonded joints such as those used in the currently examined aerial delivery system. In addition to this, a novel composite frame structure for an aerial delivery system is proposed, which would result in significant reduction of the weight of such structures and therefore allow for fuel savings to be made.

2. Materials, structure and design

The system under consideration (the aerial delivery system) is shown in Figure 1. This proposed structure involves composite tubes connected via aluminium connectors. This design provides a reduction in weight alongside enhanced strength and durability.

Figure 1. The aerial delivery system.

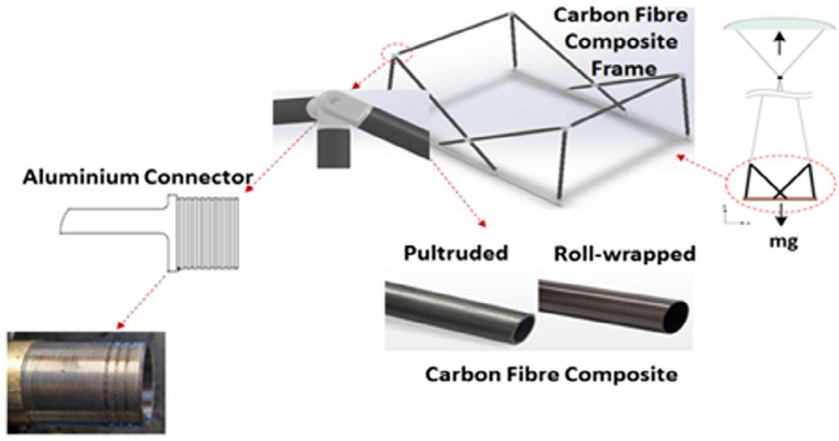

The thickness of each tube consists of five alternating composite layers of carbon and glass fibres. For better joint properties, an adhesive layer was employed at the interface between the tube and the aluminium connector. The various parameters of the utilised materials will be discussed in the paper.

2.1. Carbon fibre composite tubes

The tubes utilised in this study were predominantly manufactured using high modulus (T700) unidirectional pre-preg carbon fibre oriented to provide maximum strength in the longitudinal (lengthways) axis. In addition to this the use of pre-preg reinforcement oriented at 90° also ensures that the tube has good crush-strength; ideal for real-world applications. The use of unidirectional fibres and maximum strength in the longitudinal axis does mean that the tube is not as strong across its diameter as it is along its length so should be used in such a way as to avoid unnecessary crushing forces across the tube. The phrase "roll wrapped" refers to the process used to manufacture these tubes. The pre-preg carbon fibre is first laid up around a mandrel in multiple layers. Once the reinforcement is in place it is spiral wrapped with heat-shrink tape (this is what gives roll-wrapped tubes their characteristic ribbed appearance) before the whole assembly is oven cured. Roll wrapped carbon fibre tubes offer superior strength in general use to "pultruded" tubes (which have all their fibres running in exactly the same direction). This is because forces on a tube are rarely exclusively in straight compression or tension, whereby the unidirectional fibres of a pultruded tube are not ideal. This difference between the pultruded and the roll-wrapped tubes is illustrated in Figure 2.

The specifications of the roll-wrapped tube proposed for this application are listed in Table 1.

Figure 2. Pultruded and roll-wrapped tubes.

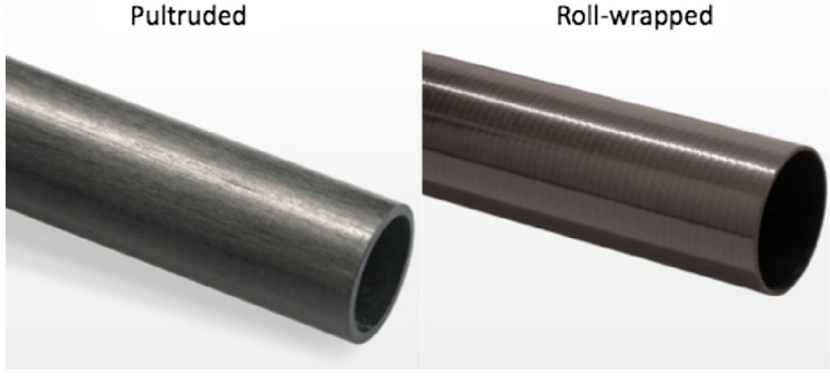

Table 1. Specification of the proposed roll-wrapped tube

Internal diameter (mm)	Wall thickness (mm)	Outer diameter (mm)	Stiffness (KN/m²)	Weight (kg/m)
50.8	1.6	54.0	9.17	0.45

Table 2. A comparison between the roll-wrapped tube with aluminium and steel tubes

Property	The proposed roll wrapped carbon fibre tube	Steel	Aluminium
Density (g/cc)	1.60	8.0	2.7
Youngs modulus 0° (GPa)	90	207	72
Youngs modulus 90° (GPa)	19	207	72
In-Plane Shear modulus (GPa)	4.6	–	–
Major Poisson's ratio	0.14	–	–
Ult. tensile strength 0° (MPa)	750	990	460
Ult. comp. strength 0° (MPa)	600	990	460
Ult. tensile strength 90° (MPa)	400	990	460
Ult. comp. strength 90° (MPa)	350	990	460

The roll wrapped carbon fibre tubes are manufactured from special high-modulus Toray T700 unidirectional pre-preg carbon fibre oriented at 0° (down the length of the tube). Crush/burst strength is provided by unidirectional E-Glass oriented at 90° (around the section of the tube). Each tube is made of five layers arranged in a 0°, 90°, 0°, 90° and 0° layup where the 0° layers are 300 gsm carbon fibre Toray T700 layers and the 90° are 300 gsm E-Glass ~ UD (80/20). The differences in material properties of the roll-wrapped tube made of carbon fibre and tubes made of Aluminium and Steel are shown in Table 2. The manufacturing tolerances are ±0.2 mm for the "Inner Diameter" and ±0.3 mm for the "Outer Diameter". In this table, it can be seen that a great reduction in density (~5 times less) is achieved through replacing the steel members by carbon fibre tubes. The strength and stiffness of steel is greater than that of the carbon fibre material, however, the reduction in density compensates for the slight reduction in these properties.

2.2. Aluminium connector

The aluminium connector is manufactured with grooves, which look like threads, machined in order to allow more adhesive to be added at the interfacial area as shown in Figure 3. The depth of the grooves is about 1 mm which means that the interfacial thickness between the aluminium and the carbon fibre tube's inner surface varies between 0.2 and 1.2 mm which is filled with the adhesive material when in the proposed joint with the carbon composite tubes.

In this study the aluminium connectors were manufactured from aluminium alloy 6082-T6. This alloy is a medium strength alloy with excellent corrosion resistance. It has the highest strength of

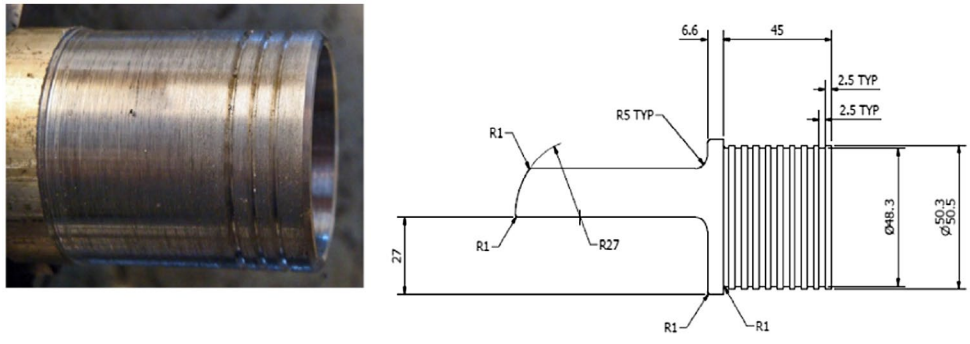

Figure 3. The proposed aluminium connector.

Table 3. The chemical composition of aluminium 6082

Element	Present (%)
Silicon (Si)	0.70–1.30
Magnesium (Mg)	0.60–1.20
Manganese (Mn)	0.40–1.00
Iron (Fe)	0.0–0.50
Chromium (Cr)	0.0–0.25
Zinc (Zn)	0.0–0.20
Others (Total)	0.0–0.15
Titanium (Ti)	0.0–0.10
Copper (Cu)	0.0–0.10
Other (Each)	0.0–0.05
Aluminium (Al)	Balance

the 6000 series alloys and is widely used as a structural material. As a relatively new alloy, the higher strength of aluminium 6082 has made it a good choice for the replacement of conventional aluminium 6061, in many applications. The addition of a large amount of manganese controls the grain structure which in turn results in a stronger alloy. It is difficult to produce thin walled, complicated extrusion shapes in alloy 6082. The extruded surface finish is not as smooth as other similar strength alloys in the 6000 series. In the T6 and T651 tempered varieties, alloy 6082 machines well and produces tight coils of swarf when chip breakers are used. General applications of this class of aluminium include highly stressed applications, trusses, bridges, cranes and transport applications. The chemical composition is shown in Table 3.

The properties of this grade of aluminium are listed in Table 4.

2.3. The adhesive material

The adhesive considered in this study is Permabond® ET5428 BLACK which is a thixotropic two part (A and B) adhesive with excellent resistance to impact and vibration. The controlled flow properties as well as its ease of mixing and application, enables the adhesive to be used where gap filling is required. Permabond® ET5428 BLACK has been found to provide exceptional performance even at elevated temperatures. Permabond® ET5428 BLACK has been specifically formulated for use in applications requiring toughness and high strength and shows benefits in the construction of composite assemblies. The physical properties of this adhesive are summarised in Table 5.

The typical curing properties are also summarised in Table 6.

Table 4. The properties of aluminium 6082

Property	Value
Density	2.70 g/cm^3
Thermal expansion	24 × 10^{-6}/K
Thermal conductivity	180 W/m ·K
Melting point	555°C
Modulus of elasticity	70 GPa
Electrical resistivity	0.038 × 10^{-6} Ω ·m
Proof stress	240–255 MPa
Tensile strength	275–300 MPa
Elongation at fracture	6–9%

Table 5. The physical properties of permabond ET5428 BLACK adhesive

Category	ET5428BLACK (Part A)	ET5428BLACK (Part B)
Chemical composition	Epoxy resin	Polyamine hardener
Appearance	White	Black
Mixed appearance	Charcoal black	
Viscosity @ 25C	25,000–35,000 MPa. S	15,000–20,000 MPa. S
Specific gravity	1.14	1.07

Table 6. Curing properties of permabond ET5428 BLACK adhesive

Mix ratio	2:1 by volume (100:48 by weight)
Maximum gap fill	5 mm (0.2in)
Usable/Pot life @23 C 10 g mixed	10 min
Time to achieve working strength	23C: 1 h, 60C: 15 min.
Time to achieve full cure	23C: 72 h, 60C: 1 h

Table 7. The mechanical properties of the cured adhesive

Shear strength (ISO 4587)	Mild steel: 18–22 N/mm^2
	FRP Glass/Polyester: 6–9 N/mm^2
	FRP Glass/Epoxy: 24–28 N/mm^2
	Carbon Fibre: 20–38 N/mm^2
Peel strength (Aluminium)	150–250 N/25 mm

The performance of the cured adhesive with some common materials is shown in Table 7. The strength results will vary depending on the level of surface preparation and gap and cure temperature.

Before applying the adhesive, the surfaces should be clean, dry and grease-free. The removal of the oxide layer off metal surfaces by lightly abrading using an emery cloth or similar is advised for metals such as aluminium and copper and their alloys.

2.4. The testing procedure

The Permabond® ET5428 BLACK adhesive was applied to the "grooved" aluminium connectors which were then inserted into the ends of the carbon fibre tube. This implies that the thickness of the adhesive varies from 0.2 mm (which is the gap between the aluminium and the inner surface of the carbon fibre tube) to 1.2 mm (at the grooves whose depth is 1.0 mm). The specimen, consisting of the carbon fibre tube and the aluminium connector, was then tested under monotonic tension as shown in Figure 4. The specimen failed at a load of about 6.3 kN (measured with a 200 kN load cell with an accuracy of ±0.1 kN). It was observed that the adhesive lost contact, or debonded, at the carbon fibre interface. This implies that the bond at the carbon fibre-adhesive interface is inferior to that at the aluminium-adhesive interface.

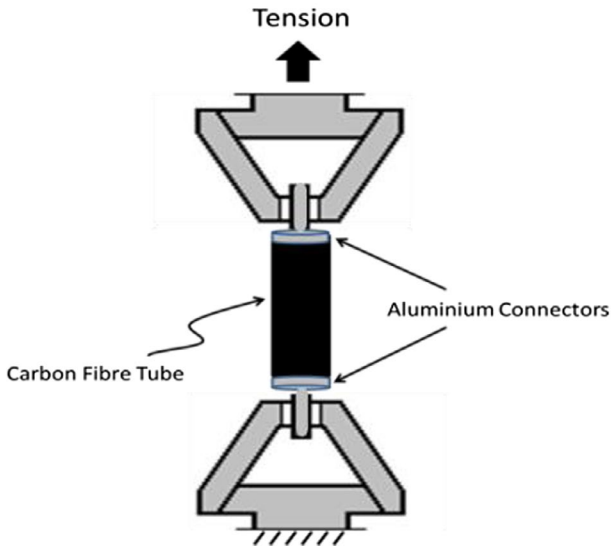

Figure 4. Schematic diagram of the tensile testing of the carbon fibre tube with aluminium connectors.

3. The contact analysis model

3.1. The modelling assumptions of the adhesive layer

The adhesive layer had a thickness of 0.2–1.2 depending on the location along the line of adhesion (either away or at the groove, respectively). The thickness of the adhesive was taken as a value between these extremes as 0.6 mm (dashed line in Figure 5). This is a simplified model that has proved to provide the same strength when practically tested.

The adhesive stiffness is a very important parameter to explore which adhesive can be used in this type of joint. In this model, the shear stiffness value K (N/mm^3) in the longitudinal directional (i.e. along the direction of the force) is given (Huveners, 2007) (Figure 6):

$$K = G/t \tag{1}$$

where K is the shear stiffness in the longitudinal direction in N/mm^3; G is the shear modulus of the adhesive in N/mm^2; t is the equivalent thickness of the joint in mm.

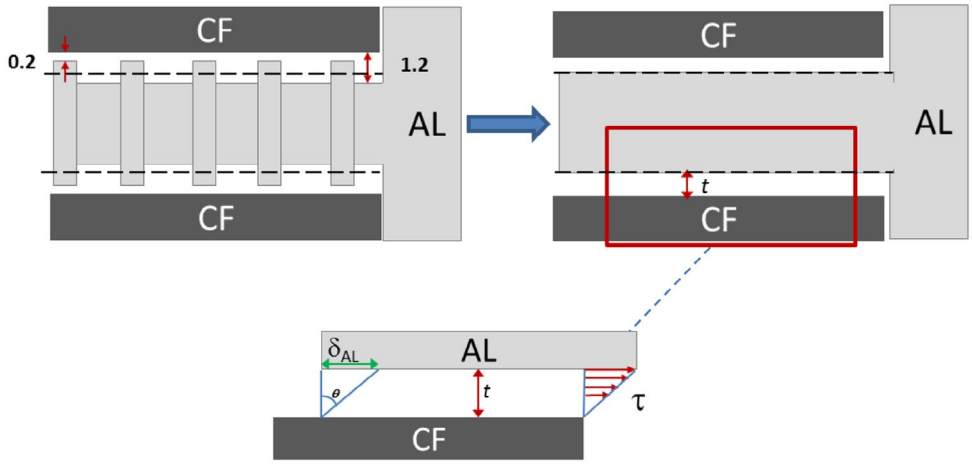

Figure 5. The actual design (left) and the simplified model (right) of the adhesive layer of t = 0.6 mm equivalent thickness.

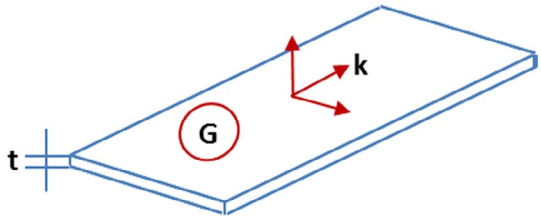

Figure 6. The adhesive layer alongside the associated stiffness.

3.2. Description of the FE model

ANSYS Workbench and ANSYS Composite PrepPost (ACP) using ANSYS Parametric Design Language (APDL) commands are the software packages which have been employed in this study to model the joint area between the carbon fibre tube and the aluminium connector. In this context, a 3D simplified geometry has been used for the numerical analysis rather than the actual geometry utilised in the lab in order to obtain the required convergence, since it is extremely difficult to represent each groove with the necessary mesh due to the small elements that would be required. In order to start the numerical analysis, CONTA174 and TARGE170 elements were used to simulate the adhesive layer. These two element types represent the sliding behaviour between the 3D targeted surfaces along with the deformation features of the surface. The location of such elements on the relevant surfaces of the 3D model are termed SOLID186 and SOLID187. They have the same geometric characteristics as the solid element face with which they are connected. Such elements allow the separation of the bonded contact to simulate the delamination of the interface. Moreover, they are considered higher order elements that are able to provide more accurate results for quadrilateral mesh and can tolerate irregular shapes without much loss of accuracy. The 20-node elements have compatible displacement shapes and are well suited to model such a joint. The Pure Penalty Method (penetration and no sliding) (ANSYS, 2010; Doyle, 2012; You, 2013) has been used in the tangential direction while using the conditions of the Lagrange Multiplier method which involves sliding with no penetration according to ANSYS (2010):

$$F_{\text{tangential}} = K_{\text{tangential}} \cdot X_{\text{sliding}} \tag{2}$$

where $F_{\text{tangential}}$ is the tangential force between the surfaces, $K_{\text{tangential}}$ is the tangential stiffness between the surfaces and X_{sliding} is the sliding distance as a result of the applied force. The value of X_{sliding} is ideally zero for sticking conditions, however, some slip is allowed in our case. This will require chattering control parameters as well as a maximum allowable elastic slip (ELSI) parameter (i.e. $K_{\text{tangential}}$) (Doan, 2013).

The accuracy of the results was improved using geometry as well as material non-linear analysis. The joint has shear failure mode which is the debonding between the Carbon fibre tube and the Aluminium. For this reason, the failure loads were predicted using this analysis. In this section, a brief description on modelling of the failure modes is presented.

3.2.1. Shear failure and the debonding between the connector and the tube

In addition to the above boundary conditions, the "cohesive zone material" model has been used to model the delamination process of the interface (i.e. debonding). The adhesion properties of the utilised adhesive were entered via the "cohesive zone material model" with "bi-linear" behaviour mode and these were allocated for the contact elements of the model. To define a bi-linear material's behaviour of adhesion, the separation distance and the constant properties of the adhesive material, the TBDATA command in ANSYS was used. In this case, five constants need to be determined by the user, namely: the maximum normal stress σ, the gap at the completion of debonding u_n^c, the maximum tangential stress τ, the tangential slip at the completion of debonding u_t^c and the artificial damping coefficient η (ANSYS, 2009, 2012).

This paper defines the process of separation of the interfacial surfaces where a tangential slip dominates the separation process in a direction parallel to the interface. The tangential stress and

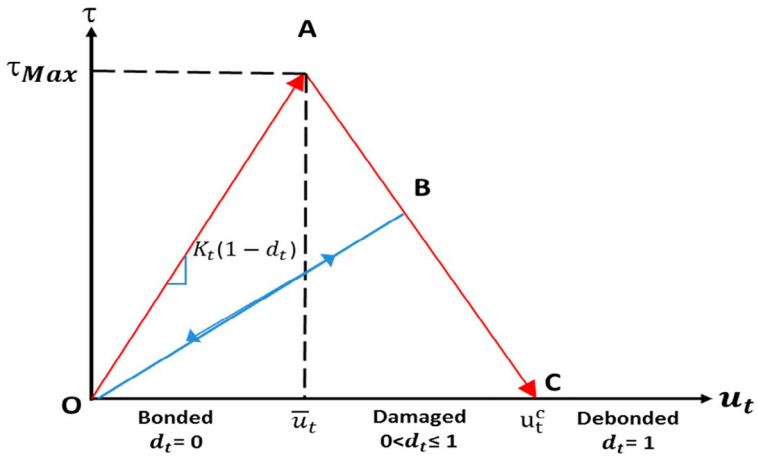

Figure 7. The tangential contact stress against slip distance for the cohesive zone material.

the slip distance were numerically modelled. When plotting the tangential contact shear stress τ against the tangential slip distance (u_t), it can be seen that there is a linear elastic loading region from point O to A and a softening or debonding region from point A to C. In this case, the contact shear stress reaches a maximum value, τ_{max}, at point A where the corresponding tangential slip distance is denoted $\bar{u}_t$. Afterwards, a drop in the slope is observed emphasising that a separation is taking place until point *C* is reached, whereby the tangential slip distance reaches u_t^c at zero shear stress value. The debonding process is approached. In the same manner, after point A, any unloading or reloading will follow the line OB since plastic strain accumulates and no longer will follow the line OA. The slopes of OA and OB are defined in Figure 7.

The equation for the maximum tangential contact stress τ_{max} and tangential slip distance $\bar{u}_t$ is written as:

$$\tau_{max} = K_t(1 - d_t)\bar{u}_t \tag{3}$$

where K_t is the tangential contact stiffness, $\bar{u}_t$ is the tangential slip distance at the maximum tangential contact stress and d_t is a damage parameter Ansys manual (ANSYS, 2012). At the completion of debonding, a slip distance u_t^c is reached (input data) and further continues to a value u_t which is the total slip distance. The slope is given by:

$$\text{Slope} = K_t(1 - d_t) \tag{4}$$

The debonding mode is based on the input data, Mode is used for tangential data (input via the TBDATA command: the tangential contact stress, τ and the tangential contact stiffness K_t. The artificial damping effect is used to facilitate the convergence of the numerical solution during modelling). In other words, debonding is accompanied by convergence difficulties when the Newton–Raphson solution method is employed. The artificial damping effect is used to overcome such problems. The damping coefficient, η, has the same units as those for time. The value of the damping coefficient should be smaller than the "minimum time step size" so that the maximum traction and maximum separation values are not exceeded during the debonding calculations. The damping coefficient η can be input via the TBDATA command using TB, CZM.

4. The simplified geometry of the validating model

The model was carried out using Mode wherein a tangential stress along with a slip distance is numerically modelled. The composite tube was modelled using a shell element whereas the aluminium connector was modelled via a solid element. The resin, in the composite, is subjected to a "pull-out" force leading to delamination of the resin layers within the composite. The adhesive layer

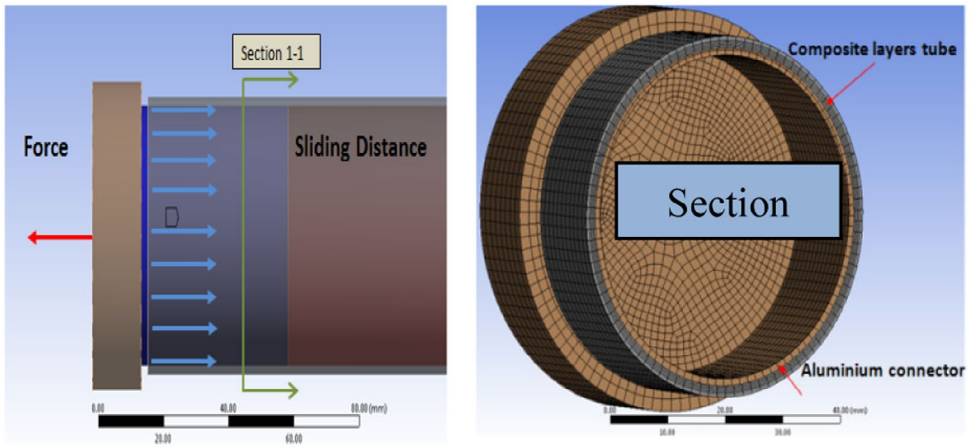

Figure 8. The adhesive layer model.

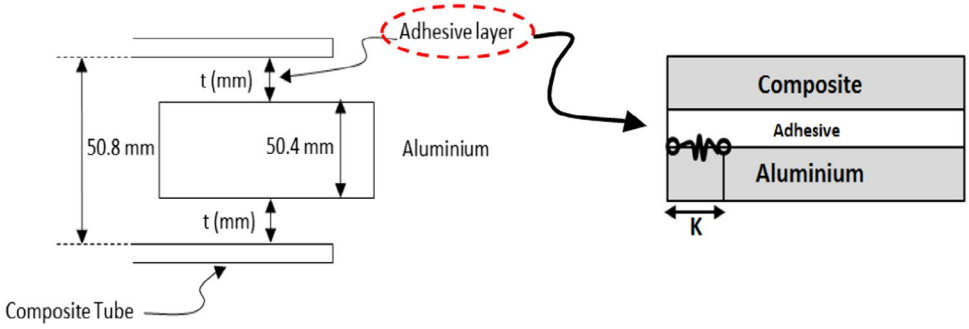

Figure 9. Detail of composite aluminium adhesive joint.

between the aluminium and the composite is very stiff (stiffness coefficient *K*) and suffers from less elongation and, therefore, can be modelled as a "Cohesive Zone" layer using Mode tangential debonding scenario Figure 7. The type and properties of the adhesive were supplied by Airborne Systems UK. The aluminium connector of an outer diameter of 50.4 mm is inserted inside the composite tube which has an internal diameter of 50.8 mm.

The length of the composite tube is 500 mm and the thickness of the tube is 1.71 mm composed of 5 layers of carbon and glass fibres arranged in 0°, 90°, 0°, 90°, 0° layout as shown in Figure 8.

One main difference between the experimental and the ANSYS workbench results was that the ANSYS simulation allowed the specimen to continue sliding after it had met the converged debonding force whereas in reality both the force and the sliding distance are reduced to zero immediately after debonding. The debonding force in the numerical simulation was about 6.7 kN at which the solution has reached its maximum convergence. This is due to the fact that the model will assume the behaviour of the structure as a "spring" which is the assumption for the adhesive layer. This has resulted in differences between the experimental and numerical solutions as shown in Table 8. It is acknowledged that errors are generated in the numerical model when the adhesive contact enters the plastic region. The main factor causing discrepancy between the experimental and numerical results was the use of a cohesive failure pattern to model the adhesion failures in the experiment.

Table 8. The experimental and numerical results

Parameter	Experimental value (KN)	Numerical model prediction (KN)	Error (%)
Debonding force	6.3	6.7	6.34

4.1. Uncertainty analysis

In structural analysis, it becomes essential to determine the relationship between the various parameters with respect to the component geometry, the applied load, the material properties, and the contour conditions. In general, the main sources of uncertainty are associated with the properties of the adhesive, the geometry, material, fibre orientation, etc. (Neto & Rosa, 2008). In the current paper, the properties of the adhesive have been considered for the analysis. In particular, parameters such as the thickness of the adhesive layer and the properties of the adhesive such as the shear strength will be investigated. This will allow a matrix of all properties and the frequency of debonding occurrence at each corresponding condition to be constructed. This will also provide a measure of the sensitivity of each parameter on the debonding force in such a structure.

4.2. Robust design under uncertainty

Research studies by Bryne and Taguchi and colleagues represent the first efforts in developing robust designs. They have introduced methods to minimise the effect of uncontrollable parameters during the design stage (Bryne & Taguchi, 1987; Taguchi, 1989). Further studies by Ross and colleagues employed the Taguchi loss function to make the design more tolerable to model variations (Ross, 1995). Other researchers proposed methods to reduce the variations in input parameters to obtain designs with lower sensitivities to design parameters (Ramakrishnan & Rao 1991). They have suggested a method for robust design with the Taguchi loss function as the object that is subjected to the model constraints. This allows the constant and variable sensitivities from controllable and uncontrollable parameters to be reduced using non-linear analysis. On the other hand, Padulo has investigated two main approaches for robust optimization in which the parameters are stochastic. The purpose of uncertainty in this case was to identify the uncertainties in input and output of a system or simulation tool (Padulo, Forth, & Guenov, 2008). In this paper, the numerical model is a detailed FE model that includes 17,179 elements as shown in Figure 8 and its computational cost was extremely expensive. In the first step, 1,000 samples have been generated from the space of input parameters and a Monte Carlo simulation run to find the corresponding 1,000 outputs, i.e. debonding force and sliding distance. The considered parameters used for uncertainty propagation include the followings: the thickness of the adhesive, the shear modulus of the adhesive, the strength of the adhesive, and the ratio between u_t and $\bar{u}_t$, Figure 7, where u_t is the slip distance when the debonding process is almost complete at which point the shear approaches a zero value and $\bar{u}_t$ is the slip distance when the shear stress reaches its maximum value.

In the current study, uniform distributions are assumed for the input parameters. The realistic lower and upper bounds of the parameters have been found elsewhere in similar studies (Huveners, 2007). The Monte-Carlo simulation was used to generate 1,000 adhesive properties after which they were run using ANSYS. The aforementioned process will automatically be carried out using a recently developed in-house MATLAB code that has been created during the course of the current project. The average time of each run required about 777.6 s.

Then, the Kernel probability distribution function has been estimated from sample data using the ksdensity function in MATLAB (R2013b). Regions of acceptable outputs, sliding distance and debonding force, are defined and samples from these regions are taken to plot Pareto curve and determine the best compromising solutions (Pareto non-dominance set). After finding the optimal parameters, a Gaussian distribution is assumed for each optimal parameter (optimal parameters selected from Pareto curve) and this is propagated through the numerical model using mean-centered first order perturbation technique (Huang & Du, 2008; Khodaparast, Mottershead, & Friswell, 2008). The propagation of uncertainty requires the calculation of covariance matrix. The derivatives were determined using the "forward finite difference method". The FE model has been run for $(m + 1)$ times to fit the model wherein the value of delta used in the analysis was pre-defined as 0.1. For small uncertainty, the uncertain output vector, z, is expanded about the mean value of uncertain input parameters as:

$$z = z(\bar{\theta}) + \sum_{i=1}^{m} \left.\frac{\partial z}{\partial \theta_i}\right|_{\theta_i=\bar{\theta}_i} \left(\theta_i - \bar{\theta}_i\right) + \sum_{i=1}^{m}\sum_{j=1}^{m} \left.\frac{\partial z}{\partial \theta_i \partial \theta_j}\right|_{\substack{\theta_i=\bar{\theta}_i \\ \theta_j=\bar{\theta}_j}} (\theta_i - \bar{\theta}_i)(\theta_i - \bar{\theta}_j) + \cdots \tag{5}$$

By truncating after the first-order term,

$$z = z(\bar{\theta}) + \bar{S}(\theta - \bar{\theta}) \tag{6}$$

where $S \in \mathfrak{R}^{n\times m}$ is sensitivity matrix (n is the number of outputs and m is the number of uncertain input parameters), $\bar{\theta} \in \mathfrak{R}^{m}$ is the vector of mean input parameters. By using the mean-centred first order perturbation technique, the mean vector and the covariance matrix of outputs are calculated as:

$$\bar{z} \approx z(\bar{\theta}) \tag{7}$$

$$\mathrm{Cov}(z, z) = \bar{S}\mathrm{Cov}(theta, \theta)\bar{S}^{T} \tag{8}$$

The new advancement in the current paper is the creation of an automated script file that allows the designer to modify the parameters of complex geometries without the need to work with the Ansys environment. That is to say, the Matlab and Ansys workbench interact with each other and the parameters are modified following this approach. This allows more flexibility to deal with complex geometries as this was, in the past, only restricted to simple designs. The framework for robust design, proposed in this paper, is summarised in Figure 10 wherein a flow diagram describes the sequence of processes using this approach. The proposed framework will allow the designer to choose the best robust optimal parameters that result in minimum variation of objective function as will be shown in sequel.

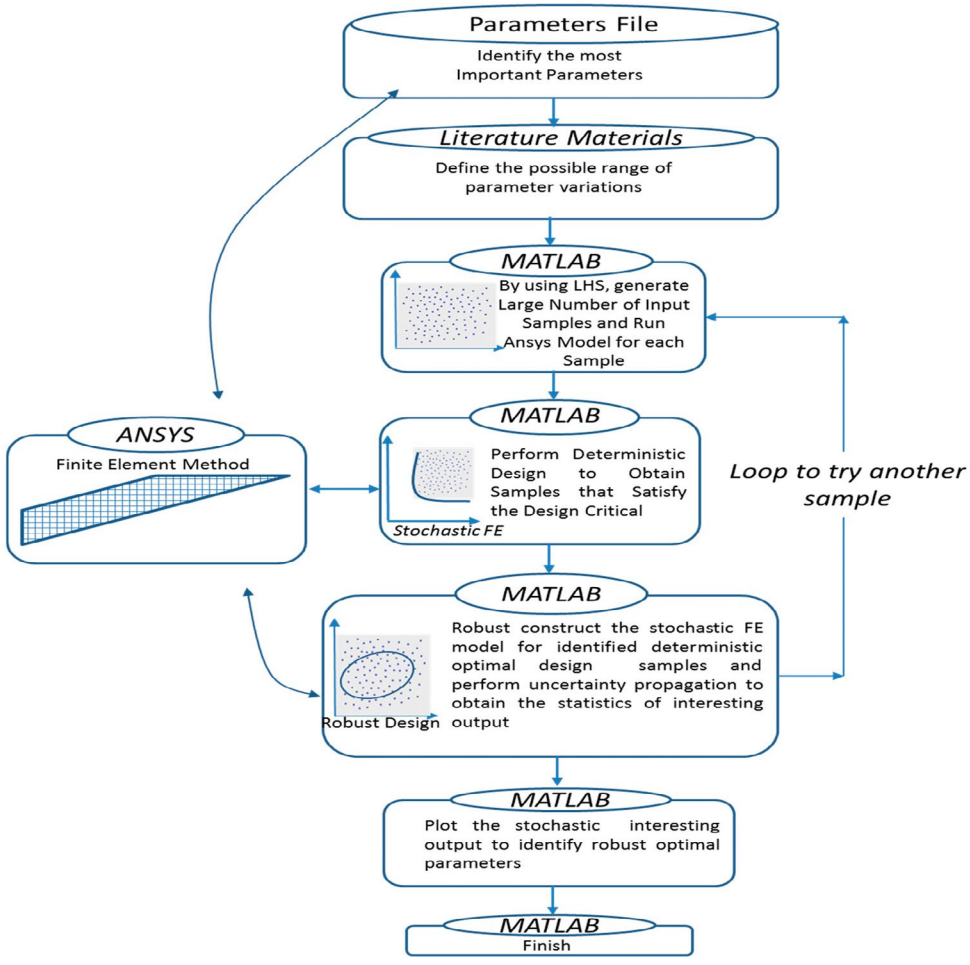

Figure 10. A flow diagram showing the sequence of processes used in this approach.

4.3. Input parameters characterization

The sources of uncertainty in the current problem are the design parameters which are subjected to variation about their nominal values such as the thickness as well as the properties of the adhesive layer (Olmi, 2012). The main aim of the current study is to evaluate the strength, thickness, shear modulus and the slip distance of the joint structure. The optimal solution is to maximise the bond strength which is desirable for real-life applications. The variability of such adhesive properties will lead to an under or over-estimation of the solution; the reason behind carrying out such an uncertainty study. The variability of debonding is dependent on the associated uncertainties during modelling. There are parametric and non-parametric uncertainties in addition to the propagation of such uncertainties throughout the model which might result in inaccurate estimations.

Several types of uncertainties might be encountered in a physics-based computational model such as; (a) Parameter Uncertainty (uncertainty in geometric parameters, friction coefficient, strength of the materials involved); (b) Model Uncertainty (arising from lack of scientific knowledge about the model); and (c) Experimental Errors (uncertain and unknown errors existing in the model when they are calibrated against experimental results) (Giorgio, 2014). These uncertainties must be assessed and managed for credible computational predictions. Due to the lack of information from the actual experiment that has been carried out (i.e. no force-displacement curve for the tensile test was recorded due to the difficulty of attaching an extensometer to the structure that has been tested, which only allowed the debonding load to be recorded), some parameters will be assumed to allow the debonding force to be evaluated and compared to the actual result. In other words, a trial and error exercise will be conducted until the modelling results show a close convergence towards the actual experimental result obtained, i.e. a debonding force of about 6.3 kN.

In Table 9, the thickness (t) of the adhesive was assumed as 0.6 mm with a proposed shear modulus of 0.011 GPa. The tangential contact stiffness K_t has been calculated by dividing the shear modulus (G) by the thickness (t) whereas the strength (S) was assumed as 3 MPa. The tangential slip distance $\bar{u}_t$ can then be obtained with the aid of Figure 7. The ratio (R) between u_t and $\bar{u}_t$ is assumed as two from which u_t can be evaluated. It is worthwhile mentioning that these are only preliminary values of the parameters with which the analysis can start in order to obtain the exact actual value of the debonding force (i.e. 6.3 kN). Accordingly, the correct parameters can be utilised to study the sensitivity of the model and to carry out the necessary uncertainty exercises.

Table 9. Input parameters characterization

Item	Type
Thickness (t), mm	Parameter
Shear modulus (G), GPa	Parameter
Tangential contact stiffness (k_t), GPa/mm	Non parameter
$k_t = G/t$	
Strength of adhesive (S), MPa	Parameter
$\bar{u}_t = S/k_t$, mm	Non parameter
R	Parameter
$u_t = \bar{u}_t \times R$, mm	Non parameter

5. Results and discussion

This paper estimates the robust design using the interface between MATLAB (to input the design parameters) and ANSYS (to find the corresponding result). The settings of the project application were prepared in Workbench (ANSYS toolbox) and an ANSYS script was written using text creation software such as Notepad. The batch, or script, file for running the ANSYS code was saved in MATLAB's working directory. To generate the interface between ANSYS and MATLAB, another script is needed to control the running of both programs in addition to the transfer of data between them. The script file of MATLAB was written to run the ANSYS Workbench. In script file, the post processing has been included to provide specific results using different function to provide the results in a vector format.

The obtained results from the uncertainty analysis and the frequency of occurrence of events are shown in Figures 11 and 12. These distributions, obtained using the aforementioned ksdensity function in MATLAB, take into account the variation in the input properties of the adhesive and the probability of debonding under each corresponding input parameter (i.e. sliding distance, reaction force and friction stress). The effects of the sliding distance studied are shown in Figure 11. It is evident that the member will have the likelihood of debonding at a distance in the range of 15–44 mm (the total joint's length is 45 mm). More pronouncedly, the highest probability of debonding will take place at about 30–33 mm sliding distance which is about 67–73% of the total joint's length. This suggests that when the sliding exceeds the mid-point of the total joint's length, the probability of debonding remarkably increases. The acceptable level for debonding in this study was assumed as 40 mm (about 90% of the total joint's length). Also above this level, the probability of debonding becomes less sensitive to the variability of the adhesive properties. This means that the properties of the joint at this level are satisfactory and reliable in the design. In other words, the properties of the samples which have provided a sliding distance of at least 40 mm were also convergent and stationary. For this reason, these were considered the optimum and acceptable level of properties provided by the simulated samples.

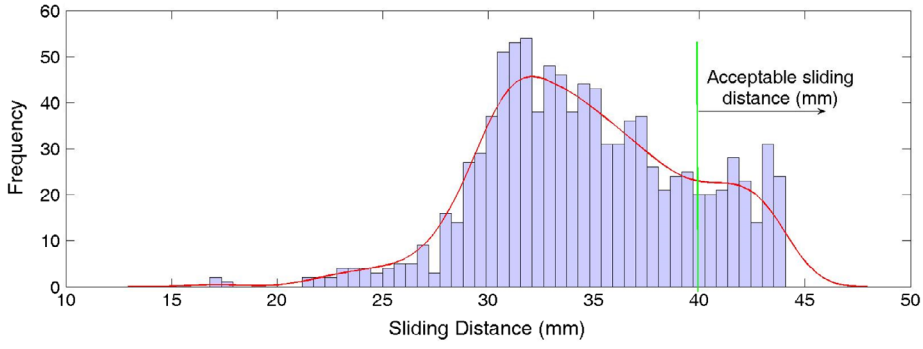

Figure 11. Frequency distribution and normality plot of the sliding distance when considering uncertainty in all parameters.

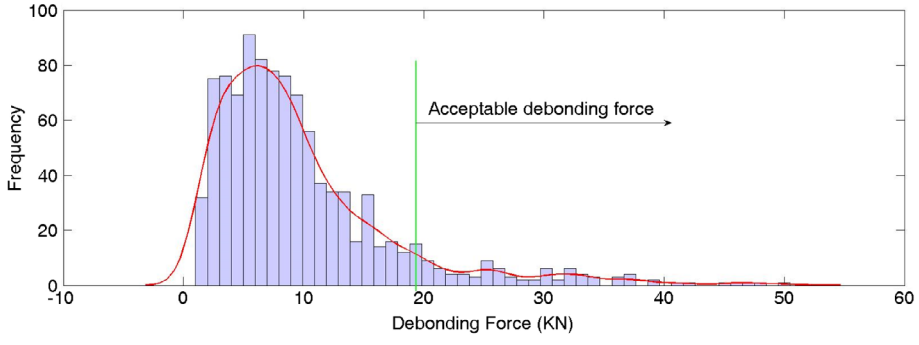

Figure 12. Frequency distribution and normality plot of the reaction force when considering uncertainty in all parameters.

The effect of the reaction force also shows that when the reaction force is as small as 1.4 KN, there will be a possibility of debonding as shown in Figure 12. However, the highest probability of debonding takes place at about 6.5 kN which is in good agreement with the experimentally achieved value of 6.3 kN. This means that the modelling results show that when the adhesive properties vary, they are most likely to debond in the aforementioned region. In order to reduce the possibility of debonding, the reaction force can be improved by improving the joint properties (adhesive strength, gap width, etc.). The acceptable level for the debonding force was assumed to start at 20 kN after which the debonding force becomes less sensitive to the change in the adhesive properties. This means that the properties of the samples that have achieved a debonding force of 20 kN and above were stationary and convergent. This means that such a level of properties will provide the optimum and acceptable performance of the joint.

5.1. Robust design under uncertainty

From Figures 11 and 12, the values of the acceptable levels of adhesive properties in terms of the debonding force and sliding distance were identified and collected. Each value of these represents a random sample of the adhesive properties that provides a certain sliding distance and debonding force when modelled. In other words, these adhesive properties have provided a higher than 20 kN debonding force and more than 40 mm sliding distance which is desirable. The inverse of the sliding distance was plotted against the inverse of the corresponding debonding force of each variant of the selected adhesive properties as shown in Figure 13. The shape of the obtained results takes an "*L*" shape which includes the "deterministic and optimal design" values clustered near the corner of the curve (circled) and almost lies on the 45° line drawn on top of the graph. This graph is similar to Pareto curve that is normally used for deterministic multi-objective optimisation problems. These seven values provide the maximum debonding force and sliding distance as discussed later. This gives seven optimum adhesive properties that fulfill the required design criteria of the joint in terms of strength and reliability.

If each value of these seven deterministic properties is assumed as a mean value of the normal distribution, then there will be a possible standard deviation that provides a set of properties around that mean value. The selected standard deviation for this exercise was 0.5% from the mean value. There are two steps in the robust design analysis of the current paper. In the first step, the realistic variation of the adhesive properties are considered to identify the optimal parameters that provide acceptable levels of deboning force and sliding distance. Once those samples are identified, i.e. the seven samples shown in Figure 13, then the objective would be to find these samples which not only maximizes the debonding force and sliding distance, but are also robust with respect to variation in their properties. A standard variation of 0.5% is chosen for the second step of the analysis, i.e. robust design. This small value of standard deviation can provide a closer study of the sensitivity of the robust design rather than studying the scatter of the data shown in the perturbation results. The value of 0.5 standard deviation has provided the results shown in Figure 14. The justification for the use of a small standard deviation value can be attributed to the fact that the problem is strongly nonlinear.

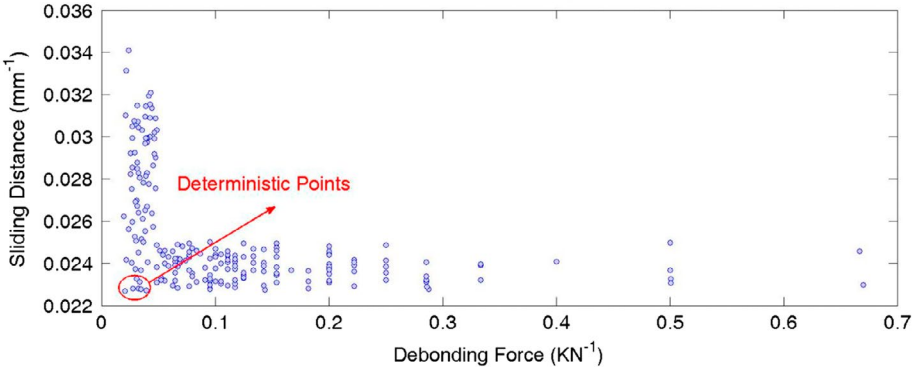

Figure 13. The inverse of the sliding distance vs. the inverse of the debonding.

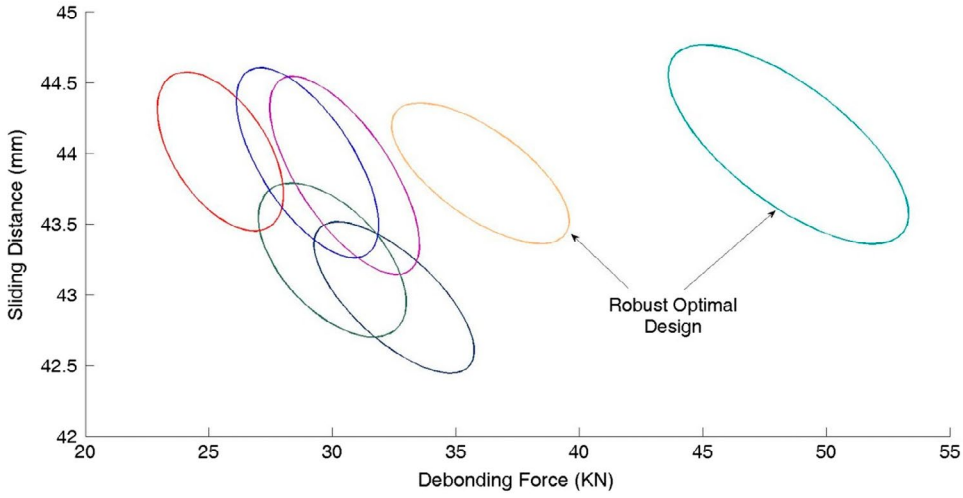

Figure 14. The Gaussian-based confidence ellipses method for the selection o the robust design.

The use of a small standard deviation ensures the reliability of the first order perturbation method. If a higher standard deviation was chosen, a second or higher order perturbation method should have been used for the uncertainty propagation. The Perturbation approach is employed to estimate the variability of outputs in the stochastic model and also to evaluate certain covariance matrices as part of the robust design procedure (Du, 2004). This method has extensively been employed and discussed elsewhere for similar design problems (Khodaparast et al., 2008).

In Figure 14, the centres of all ellipses are the seven deterministic values that were derived from Figure 13. It can be seen that the area and thus, the range of properties, of each ellipse in terms of the sliding distance and debonding force varies from one ellipse to the other depending on the utilised deterministic adhesive value. The shape of each ellipse is also dependent on the standard variation used (that is 0.5% for all ellipses) and the natural distribution of the values around the mean. In this exercise, two selection criteria can be used: The area of the ellipse (the smaller the better) and the location of the centre of the ellipse (as the centre of the ellipse approaches the upper right hand corner, the maximum sliding distance and debonding force are achieved). In the former selection criteria, the smaller the area of the ellipse, the less sensitive the adhesive to this variation. In other words, the smaller area of the ellipse provides values that are more densely concentrated around the mean (i.e. the centre of the ellipse). Whereas in the latter selection criteria, as the centre of the ellipse moves to the upper right hand corner, this will then provide the maximum debonding force and sliding distance. When taking the former selection criteria into consideration, the orange-coloured ellipse provides the most robust design since its area is the smallest and thereupon its sensitivity to any variation in properties. On the other hand, when the second selection criteria is considered, the maximum sliding distance and debonding force are achieved by the green-coloured ellipse which represents another robust optimal design. Despite the fact that its area is larger than the others and thus the adhesive properties of this ellipse are more sensitive to any change in parameters, this can be compensated by the superior mechanical properties obtained when this adhesive is utilised in the design of the joint. The input parameters that resulted in the adhesive properties represented by these two ellipses are the best candidates to be used for adhesively bonding the joints in the aerial delivery system to robustly obtain the optimum performance of the structure.

6. Conclusions

In this paper, a composite frame structure made of carbon fibre material using aluminium connectors is proposed for Aerial Delivery Systems. This results in significant reduction in the weight of the structure. The main issue in the proposed structure was the joints between members as the previous screwed fasteners could no longer be used. Instead, an adhesively bonded joint between the composite material and the aluminum connector is proposed for the structure and a framework is

suggested to obtain the optimal material and geometrical parameters of adhesive joints that not only maximize the debonding force and sliding distance, but also minimise their sensitivity with respect to any small variation in the input parameters. A MATLAB code was developed and linked with an ANSYS model to perform this exercise. The obtained results have shown that the optimum properties characterised by the maximum debonding force and sliding distance have been achieved by seven deterministic values of the randomly run properties. The Gaussian distribution was assumed for each optimal parameter and the first order perturbation method was employed. This has provided the best robust optimal parameters that have resulted in the minimum variation of the objective function.

Funding
This work was supported by Swansea University [grant number EG119].

Author details
Nada Aldoumani[1]
E-mail: n.s.f.aldoumani@swansea.ac.uk
Hamed Haddad Khodaparast[1]
E-mail: H.Haddadkhodaparast@Swansea.ac.uk
Ian Cameron[1]
E-mail: I.M.Cameron@Swansea.ac.uk
Michael Friswell[1]
E-mail: M.I.Friswell@Swansea.ac.uk
David Jones[2]
E-mail: David.Jones@airborne-sys.co.uk
Arun Chandrashaker[1]
E-mail: arunchandrashaker@me.com
Johann Sienz[1]
E-mail: J.Sienz@Swansea.ac.uk
ORCID ID: http://orcid.org/0000-0003-3136-5718
[1] The Advanced Sustainable Manufacturing Technologies (ASTUTE) Project, College of Engineering, Swansea University, Fabian Way, Swansea, SA1 8EN, UK.
[2] Airborne Systems Ltd, Bettws Road, Llangeinor, Bridgend, CF32 8PL, UK.

Citation information
Cite this article as: The robustness of carbon fibre members bonded to aluminium connectors in aerial delivery systems, Nada Aldoumani, Hamed Haddad Khodaparast, Ian Cameron, Michael Friswell, David Jones, Arun Chandrashaker & Johann Sienz, *Cogent Engineering* (2016), 3: 1225879.

References

AHN, J. (2011). Advanced modeling of the behavior of bonded composite joints in aerospace applications. In P. Camanho & L. Tong (Eds.), *Composite Joints and Connections* (p. 423). Chapter 14.

ANSYS. (2009). *Element reference*. Author. Retrieved from https://www.scribd.com/document/172048919/Ansys-Bible

ANSYS. (2010, December). *Introduction to contact, ANSYS mechanical ANSYS mechanical, lecture 3*. Retrieved May 6, 2014, from ANSYS customer training material: http://inside.mines.edu/~apetrell/ENME442/Labs/1301_ENME442_lab6_lecture.pdf

ANSYS. (2012). *ANSYS mechanical APDL theory reference*. Author. Retrieved from http://148.204.81.206/Ansys/150/ANSYS%20Mechanical%20APDL%20Theory%20Reference.pdf

Baker, A., Dutton, S., & Kelly, D. (2004). Composite materials in aircraft structures. *Industrial Engineering, 43*. doi:10.2322/jjsass1969.43.213

Bryne, D., & Taguchi, S. (1987). The Taguchi approach to parameter design. *Quality Progress, 20*, 19–26.

Campilho, R. D. S. G., Banea, M. D., Pinto, A. M. G., Da Silva, L. F. M., & De Jesus, A. M. P. (2011). Strength prediction of single- and double-lap joints by standard and extended finite element modelling. *International Journal of Adhesion and Adhesives, 31*, 363–372. doi:10.1016/j.ijadhadh.2010.09.008

Degenhardt, R. (2014). Future structural stability design for composite space and airframe structures. *Thin-Walled Structures, 81*, 29–38.

Doan, M. (2013). *Advances in ANSYS R14.5 structural mechanics solutions*, 92. Retrieved from http://www.pdfdrive.net/advances-in-ansys-r145-structural-mechanics-solutions-e1961250.html

Doyle, J. (2012, February 16). *ANSYS*. Retrieved May 3, 2014, from What Are the Differences between the Contact Formulations http://www.ansys-blog.com/what-are-the-differences-between-the-contact-formulations/

Du, X. (2004). An integrated framework for optimization under uncertainty using inverse reliability strategy. *Journal of Mechanical Design, 126*, 562–570. http://dx.doi.org/10.1115/1.1759358

Giorgio, O. (2014). Reliability assessment of a turbogenerator coil retaining ring based on low cycle fatigue data. *Mechanical Engineering, 61*, 5–34.

Harris, J., & Adams, R. (1984). Strength prediction of bonded single lap joints by non-linear finite element methods. *International Journal of Adhesion and Adhesives, 4*, 65–78. http://dx.doi.org/10.1016/0143-7496(84)90103-9

Hart-Shith, L. (1973). *Adhesive- bonded single-lap joints. Prepared under Contract NASl-ll234, Douglas Aircraft Company, McDonnell Douglas Corporation*. Long Beach, CA: Langley Research Center, National Aeronautics and Space Administration. Retrieved from http://ntrs.nasa.gov/archive/nasa/casi.ntrs.nasa.gov/19740005082.pdf

Hollaway, L. (1994). *Handbook of polymer composites for engineers*. Woodhead Publishing. http://dx.doi.org/10.1533/9781845698607

Hosseini-Toudeshky, H., Ghaffari, M. A., & Mohammadi, B. (2013). Mixed-mode crack propagation of stiffened curved panels repaired by composite patch under combined tension and shear cyclic loading. *Aerospace Science and Technology, 28*, 344–363. doi:10.1016/j.ast.2012.12.001

Huang, B., & Du, X. (2008). Probabilistic uncertainty analysis by mean-value first order saddlepoint approximation. *Reliability Engineering & System Safety, 93*, 325–336.

Huveners, E. (2007). *Mechanical shear properties of adhesives*. Proceedings of the 10th International Conference on Architectural and Automotive Glass, Finland.

Kairouz, K., & Matthews, F. L. (1993). Strength and failure modes of bonded single-lap joints between cross-ply adherends. *Composites, 24*, 475–484. http://dx.doi.org/10.1016/0010-4361(93)90017-3

Khodaparast, H. H., Mottershead, J. E., & Friswell, M. I. (2008). *Perturbation methods for the estimation of parameter variability in stochastic model updating. Mechanical Systems and Signal Processing, 22*, 1751–1773. doi:10.1016/j.ymssp.2008.03.001

Kim, K.-S., Yoo, J. S., Yi, Y. M., & Kim, C. G. (2006). Failure mode and strength of uni-directional composite single-lap bonded joints with different bonding methods. *Composite Structures, 72*, 477–485. http://dx.doi.org/10.1016/j.compstruct.2005.01.023

Kweon, J.-H. (2006). Failure of carbon composite-to-aluminum joints with combined mechanical fastening and adhesive bonding. *Composite Structures, 75*, 192–198. http://dx.doi.org/10.1016/j.compstruct.2006.04.013

Lang, T., & Mallick, P. (1998). *Effect of spew geometry on stresses in single lap adhesive joints*. *International Journal of Adhesion and Adhesives, 18*, 167–177.

Li, G., Lee-Sullivan, P., & Thring, R. W. (2000). Determination of activation energy for glass transition of an epoxy adhesive using dynamic mechanical analysis. *Journal of Thermal Analysis and Calorimetry, 60*, 377–390. doi:10.1023/A:1010120921582

Liljedahl, C. D. M., Crocombe, A. D., Wahab, M. A., & Ashcroft, I. A. (2007). Modelling the environmental degradation of adhesively bonded aluminium and composite joints using a CZM approach. *International Journal of Adhesion and Adhesives, 27*, 505–518. doi:10.1016/j.ijadhadh.2006.09.015

Mathews, F. (1987). *Joining fibre reinforced plastics*. Amsterdam: Elsevier.

Mazumdar, S., & Mallick, P. K. (1998). *Static and fatigue behavior of adhesive joints in SMC–SMC composites*. *Polymer Composites, 19*, 139–146. doi:10.1002/pc.10084

Neto, A., & Rosa, E. (2008). Parametric uncertainty analysis considering metrological aspects in the structural simulation in viscoelastic materials. *Latin American Journal of Solids and Structures, 5*, 75–95.

Olmi, G. (2012). An efficient method for the determination of the probability of failure on the basis of LCF data: Application to turbogenerator design. *SDHM Structural Durability and Health Monitoring, 8*, 61–90.

Owens, J. (2000). Stiffness behaviour due to fracture in adhesively bonded composite-to-aluminum joints. *International Journal of Adhesion & Adhesives, 20*, 47–58. http://dx.doi.org/10.1016/S0143-7496(99)00014-7

Padulo, M., Forth, S. A., & Guenov, M. D. (2008). Robust Aircraft Conceptual Design Using Automatic Differentiation in Matlab. *Advances in Automatic Differentiation, 64*, 271–280. doi:10.1007/978-3-540-68942-3_24

Pappadàa, S. (2015). Fabrication of a thermoplastic matrix composite stiffened panel by induction welding. *Aerospace Science and Technology, 43*, 314–320.

Ramakrishnan, B., & Rao, S. S. (1991). Robust optimization approach using Taguchi's loss function for solving nonlinear optimization problems. *In American Society of Mechanical Engineers, Design Engineering Division (Publication) DE*. (pt 1 ed., Vol. 32, pp. 241-248). New York, NY: ASME.

Ross, P. J. (1995). *Taguchi techniques for quality engineering: Loss function, orthogonal experiments parameter and tolerance design* (p. 329). McGraw Hill.

Taguchi, G. (1989). *Engineering in production systems*. New York, NY: Mc Graw Hill.

Tsai, M. Y., Morton, J., & Matthews, F. L. (1995). Experimental and Numerical Studies of a Laminated Composite Single-Lap Adhesive Joint. *Journal of Composite Materials, 29*, 1254–1275. doi:10.1177/002199839502900906

Villani, A. P. G., Donadon, M. V., Arbelo, M. A., Rizzi, P., Montestruque, C. V., Bussamra, F., & Rodrigues, M. R. B. (2015). The postbuckling behaviour of adhesively bonded stiffened panels subjected to in-plane shear loading. *Aerospace Science and Technology, 46*, 30–41. doi:10.1016/j.ast.2015.06.028

Xu, W., & Wei, Y. (2012). *Strength and interface failure mechanism of adhesive joints*. *International Journal of Adhesion and Adhesives, 34*, 80–92.

You, B. (2013). Contact algorithm of finite element analysis for prediction of press-fit curve. *Journal of Information and Computational Science, 10*, 2591–2600. http://dx.doi.org/10.12733/issn.1548-7741

Zou, G. (2004). An analytical solution for the analysis of symmetric composite adhesively bonded joints. *Composite Structures, 45*, 5914–5935.

Cogent Engineering **(ISSN: 2331-1916) is published by Cogent OA, part of Taylor & Francis Group.**

Publishing with Cogent OA ensures:

- Immediate, universal access to your article on publication
- High visibility and discoverability via the Cogent OA website as well as Taylor & Francis Online
- Download and citation statistics for your article
- Rapid online publication
- Input from, and dialog with, expert editors and editorial boards
- Retention of full copyright of your article
- Guaranteed legacy preservation of your article
- Discounts and waivers for authors in developing regions

Submit your manuscript to a Cogent OA journal at www.CogentOA.com